

Size Dependent Nonlinear Bending Analysis of a Flexoelectric Functionally Graded Nano-Plate Under Thermo-Electro-Mechanical Loads

A. Ghobadi¹, Y. Tadi Beni^{2,*}, H. Golestanian²

¹Mechanical Engineering Department, Shahrekord University, Shahrekord, Iran

²Faculty of Engineering, Shahrekord University, Shahrekord, Iran

Received 3 September 2019; accepted 8 December 2019

ABSTRACT

The effects of flexoelectricity on thermo-electro-mechanical behavior of a functionally graded electro-piezo-flexoelectric nano-plate are investigated in this paper using flexoelectric modified and the Kirchhoff classic theories. Moreover, using the variation method and the principle of minimum potential energy for the first time, the coupled governing nonlinear differential equations of the nano-plate and their associated boundary conditions are obtained. The functionally graded nano-plate is modeled using a power law equation along the plate thickness direction. The nano-plate behavior is analyzed under mechanical, electrical, and thermal loadings with different boundary conditions. It should be noted that the direct and reverse flexoelectric effects under different loading conditions were investigated. Finally, the important quantities such as: the nano-plate deflection, the induced electrical voltage for different values of the length parameter, the power index related to the functionally graded behavior model and the geometric ratio parameter are determined. The results indicate that in the presence of flexoelectricity, the rigidity of the nano-plate increases. Also, the deflection and the generated electric potential along nano-plate thickness decreases. Finally, induced polarization decreases as a linear temperature variation is applied on the nano-plate.

© 2020 IAU, Arak Branch. All rights reserved.

Keywords: Piezo-flexoelectricity; Functionally graded nano-plate; Theory of flexoelectricity; Size effect; Thermal effect.

1 INTRODUCTION

IN recent years, researchers have paid much attention to the use of the micro-electromechanical systems (MEMS), which have important applications in the mechanical, chemical and aerospace industries. As these materials have electro-mechanical behavior, they are able to convert mechanical energy (tension, pressure, buckling, and torsion) to electrical power (voltage, electric field, and electrical polarization). Thus, these materials can be used in transducers,

*Corresponding author. Tel.: +98 38 32324438.
E-mail address: tadi@eng.sku.ac.ir (Y. Tadi Beni).

including nano-transducers, nano-sensors [1], nano-actuators, nano-resonators [2], and nano-energy absorbents. Materials with a central non-symmetric molecular structure which can be electrically bipolar in response to uniform mechanical strain, are called piezoelectric materials. All dielectric materials with center-symmetrical crystalline structure are electrically bipolarized under non-uniform mechanical strain or strain gradient. This strain gradient results in an induced electrical potential in these materials. This electromechanical effect is known as the flexoelectricity phenomenon, first discovered by Cogan [3]. Experimental observations and molecular dynamics (MD) simulations have shown that mechanical properties and piezoelectric coefficients depend strongly on the length scale parameter. Thus, reducing the structure dimensions to the nano-scale, the structural properties change strongly [4]. So far, many efforts have been made to determine the flexoelectric coefficients of materials. For the first time, Kogan estimated these coefficients for some dielectrics with various crystals [5]. Marangati used general flexoelectric theory to estimate the flexoelectricity coefficients of dielectrics which indicate bipolarization due to the strain gradient [6]. This investigator used theoretical and experimental approaches to show that a non-uniform strain could eliminate the symmetry of the crystalline structure in piezoelectric materials and generates electric bipolarity in them. Hu and Shen developed the variation principle for determining the electric enthalpy energy in nano-dielectrics by taking into account the flexoelectric effect, size effects, and electrostatic force effects. They divided the electrostatic stress into two parts. A part is related to the polarization and strain tensor and another part is related to polarization gradient and strain gradient [7]. Yan investigated the effects of flexoelectricity on the electrostatic vibrational and flexural behavior of Timoshenko and Euler-Bernoulli nano-beams by considering the size effects and various boundary conditions using the Hamilton's principle. He showed that the flexoelectric effect plays an important role on the electromechanical behavior of the beams with small thicknesses [8-9]. Li et al. proposed a new formulation for flexoelectricity theory by dividing the strain gradient tensor into two independent parts. These investigators showed that the high-order coefficients of the strain gradient tensor reduce to three [10]. Also, the relation between the strain gradient tensor and the polarization tensor is expressed only by the dilatation gradient tensor and the anti-symmetric part of the deviatoric rotary gradient tensor. It should be noted that the classic atomistic continuum mechanics theories are not suitable for analyzing the behavior of nanostructures. The reason of this fact is that continuum mechanics theories ignore the space between the atoms and the particle bonds compared to the main dimensions of the structure. Hence, the other methods such as experimental methods and molecular dynamic simulations should be used to evaluate the properties of nanostructures. However, these methods are costly and are limited to small number of atoms and time consuming. In recent years, several non-classical elasticity theories, such as nonlocal elasticity theory, modified strain gradient elasticity theory, and modified couple stress theory have been proposed to incorporate small-scale effects in nano-scale and micro-scale structures. Among these, the nonlocal elasticity theory has been widely used because of its simplicity and proper application in the nonlinear behavior of the micro and nano-structures and their high accuracy [11-12]. The piezoelectric beam and the piezoelectric plate models have been improved and expanded to determine the effects of the piezoelectricity on structure response, using flexoelectric theory. Li introduced a three layer Euler-Bernoulli beam model to investigate the piezoelectric and the size effects on the static bending and free vibrations of the nano-beam [13]. For this purpose, he used the flexoelectric theory proposed by Hadjesfandiari [14]. Liang and Shen [15] considered an Euler-Bernoulli beam model and the size effect to study the electromechanical behavior of a piezoelectric nanowire using the theory introduced by Hu and Shen [16]. The obtained deflections from their models were smaller than those obtained from the classical beam theory. Also, they claim that the coupling between the electric field and the strain gradient results in an increase in the effective electromechanical coupling coefficients. Yang studied the extensional and flexural displacement of an electrostatic plate under a large electric field using the variation method for small strains and 3D electric field. In order to determine the mechanical displacement and electric potential along the plate thickness direction, they derived the two-dimensional equations [17]. Liu et al. studied free vibrations of a piezoelectric nano-plate under thermo-electro-mechanical loadings using a non-local elasticity theory and the Kirchhoff plate model. They investigated the effects of non-local parameters, axial force, external electrical voltage and temperature variations on the nano-plate vibrations [18]. Yang and Jiang studied the surface effects on the electrostatic behavior of a piezoelectric curved nano-beam using a surface layer-based model and Young-Laplace equations. Their results showed that surface effects play a significant role in the induced electrostatic field and the response of a piezoelectric nano-beam [19]. Ke and Wang studied the non-local effects on vibrations of a piezoelectric nano-beam using the non-local Timoshenko's nano-beam theory. They derived the governing equations of the nano-beam vibration under thermo- electro-mechanical loadings, using the Hamilton's principle [20]. Zhang et al. studied the flexoelectric effects on electrostatic response and free vibrations of a piezoelectric nano-plate using a developed piezoelectric theory and the classic Kirchhoff plate theory. They showed that the flexoelectric effect is dependent on the aspect ratio in presence of the external applied electric potential [21]. Zhang and Jiang, using the developed linear piezoelectric theory, investigated the size, surface, and flexoelectric effects on the

electromechanical behavior of nano-plate. In this research, static bending and vibrations of the nano-plate were investigated using modified Kirchhoff model. They took residual surface stress, surface piezoelectric effect, and surface flexoelectric effect into account [22]. Yang et al. examined the electromechanical behavior of piezoelectric nano-plate with flexoelectric effects. These researchers derived the governing equations of the problem using the Hamilton's principle and the Kirchhoff plate theory. They also determined analytical solutions for the displacement of the plate and its natural frequencies. They considered the piezoelectric and flexoelectric effects on the static and dynamic behavior of the plate, simultaneously [23]. Considering the influence of the surface tension, Yan and Jiang studied the vibrations and the bending of a piezoelectric nano-plate using the modified Kirchhoff plate model. In this study, to determine the effects of surface stress on plate vibration and buckling, they used the piezoelectric model and the Young-Laplace generalized equations [24]. Yan and Jiang studied the vibrations and bending of a piezoelectric nano-beam under the influence of a flexoelectric and size effect. The differential governing equations of the beam behavior were determined using the expanded linear piezoelectricity theory and the Timoshenko's nano-beam model. They extracted the equilibrium equations using the principle of minimum potential energy [25]. Murmu et al. studied the vibrations of a piezoelectric nano-plate under the thermo-electro-mechanical loadings based on the Kirchhoff plate model and the nonlinear elasticity theory. They investigated the effects of non-local parameters, size effect, geometric characteristics, axial force, external electrical voltage and temperature variations on the vibrational behavior of piezoelectric nano-plate [26]. Li et al. studied buckling and free vibration of the magneto-electro-elastic a nano-plate mounted on an elastic foundation using the non-local elasticity theory. They obtained the governing equations and the magneto-electric boundary conditions of the plate using the Maxwell equations and the principle of minimum potential energy [27]. Liang et al. examined surface and flexoelectric effects on static bending of a piezoelectric nano-beam by introducing a non-classic Euler-Bernoulli beam model [28]. They also used the piezoelectricity theory for this purpose. Governing equations of the beam bending were obtained by applying the variation theory principal on virtual displacement theory. Their results indicated that bending rigidity of silicon nano-beam was larger than bending rigidity of silver nano-beam. They also claimed the flexoelectricity has a significant effect on bending rigidity of the nano-beam. In another investigation, Liang et al. investigated the size effect and the flexoelectricity effect on buckling and vibrations of the piezoelectric nanostructures [29]. The analysis and the piezoelectric nano-beam was carried out using the atomistic-continuum theory and the Euler-Bernoulli beam model. The effects of electrical and mechanical loadings, electrical field, flexoelectricity, and non-local electrical voltage on the nano-beam behavior were investigated. Their numerical results showed that the bending rigidity, Young's modulus, and critical buckling voltage depend strongly on the surface effects of piezoelectricity, the flexoelectricity effect, and the residual surface stresses. Yan and Jiang studied the effect of flexoelectric on the electrostatic field around the piezoelectric nano-cylinder under electric and mechanical loadings. In this study, considering the non-local elastic effects caused by strain gradient, the governing equations and boundary conditions of the nano-cylinder were extracted using the theoretical framework by applying the principle of minimum potential energy and the variational principle. Numerical and analytical solutions were obtained by taking into account the inverse flexoelectric effect [30]. Ke et al. examined free vibration of a piezoelectric rectangular nano-plate under different boundary conditions and electrical, mechanical, and thermal loads using nonlocal elasticity theory. They considered the plate is subjected to bi-pivot force loading, external electrical voltage, and uniform temperature variations. Differential governing equations of the nano-plate vibration were obtained using the Mindlin plate theory and the principle of minimum potential energy. The effects of nonlocal parameters, mechanical, thermal and electrical loadings, boundary conditions, and geometric characteristics on vibration of nano-plate were investigated by these authors [31]. Liu et al. discussed the thermo-electromechanical free vibration of a single layer piezoelectric plate using nonlocal elasticity theory and Kirchhoff plate model [32]. These investigators determined the effects of nonlocal parameters, axial force, external electrical voltage, and temperature variations on thermo-electro-mechanical behavior of the piezoelectric nano-plate. Liang et al. studied the buckling and vibration of flexoelectric nano-plate under mechanical loading using general flexoelectricity theory. Using the principle of variation and Kirchhoff's classic plate model, they determined the plate governing equations. Then, they obtained the critical buckling load and natural frequencies of the nano-plate [33]. Alibeigi et al., using modified couple stress theory, examined the buckling behavior of a magneto-electro-elastic nano-beam. They obtained the governing equations of the nano-beam based on the Euler-Bernoulli beam model, the nonlinear strain of Von-Karman and the principle of minimum potential energy. These investigators also examined the effects of electrical potential and temperature variations on the nano-beam thermal critical buckling load [34]. Due to the special characteristics of the functionally graded materials, many scientists have focused their researches on investigating the thermo-electro-mechanical behavior of them in recent years. Therefore, static and dynamic behavior of functionally graded nano-beams used in nano-electro-mechanical systems (NEMS) and micro-electro-mechanical systems has been investigated [35-38]. Due to the special properties of the functionally grade materials

and piezo-flexoelectric effect, the materials that have both these properties can exhibit unique behavior. Moreover, these materials can have very useful applications in sensor, actuator, and transducer manufacturing. Considering the size effects, many scientists have also studied the behavior of piezoelectric nanoscale structures considering the size effects. In these investigations, the effects of small dimensions of the structure and the piezoelectric effect on electromechanical behavior have been investigated [39-41]. Kiani et al. examined the thermal buckling of a functionally graded piezoelectric beam under thermal stresses and constant voltage. The material properties were considered to vary according to power law function along the thickness direction. They derived the beam governing equations using the Euler-Bernoulli beam model and Von-Karman non-linear displacement relations. These investigators examined the effects of the power law index, the boundary conditions, and geometry of the beam and the applied voltage on thermal buckling of the beam [42]. Kiani et al. studied thermal-electric buckling of a functionally graded Timoshenko beam using variational theory. Along the investigation, mechanical and thermal properties of functionally graded beam were modeled with a power law equation along the beam thickness direction. Thermal buckling load was determined for various length to thickness ratios and different values of functionally graded power index [43]. Ebrahimi and Barati investigated the thermo-electro-elastic free vibration of flexoelectric nano-plate using the non-local elasticity theory and Kirchhoff classic plate model. They assumed the thermal loading with uniform and linear variations along the nano-plate thickness. The governing equations and associated boundary conditions were derived using Hamilton's principle. The natural frequencies of the nano-plate were determined by solving the differential governing equations using the Galerkin's method. They showed that the natural frequencies of flexoelectric nano-plate are dependent on the parameters such as: the flexoelectricity, nonlocal parameter, surface elasticity, temperature rise, plate thickness and boundary conditions [44]. Ebrahimi and Barati studied the size-dependent electro-mechanical buckling of a flexoelectric nano-beam using the nonlocal and surface elasticity theories [45]. The nano-beam was assumed to be on a two-parameter elastic foundation with infinite linear springs and a shear layer. Applying the Hamilton's principle, the governing equations and boundary conditions were derived. The obtained results indicated the influences of nonlocal parameter, surface effects, plate geometrical parameters, elastic foundation, and boundary conditions on the buckling behavior of nano-beam. In other investigations, Ebrahimi et al. analyzed thermal buckling of functionally graded nano-plates [46], magneto-thermo-electro-mechanical buckling of piezoelectric nano-beams [47,48], free vibration of the nano-beam by considering the surface and flexoelectric effects [49] and electro-mechanical buckling of size-dependent flexoelectric nano-beam [50]. Tadi Beni developed the piezoelectric Timoshenko nano-beam theory to study bending behavior and non-linear free vibration of piezoelectric nano-beam. He applied the size-dependent piezoelectricity theory for this purpose. Using the Hamilton's principle and variational method, the governing equations and boundary conditions were extracted. He assumed that nano-beam was simply supported at two ends. The obtained results indicated that the flexoelectricity effect has a significant influence on the static bending and free vibration of nano-beam [51]. It should be noted that, there are few researches in the literature focused on studying the flexoelectric nano-plate [21, 44-49], but all of these articles investigate the flexoelectric nano-plate behavior using non-local elasticity theory of Eringen, strain gradient theory and general piezoelectric theory. While, the present study used the reformulated flexoelectric theory [10] to analyze the non-linear bending of the nano-plate. Hence, the obtained results using the present theory have a significant difference compared to those using the applied theory in the mentioned other references. Due to the above discussion and considering the previous researches, the behavior of flexoelectric nano-plate was not investigated using new modified flexoelectric theory (reformulated flexoelectric theory [10]), and, so far, the researchers have not investigated the electromechanical behavior of functionally graded nano-plate under thermal loading using this new modified flexoelectric theory. Hence, this research is considered a new study on the behavior of these nano-plates.

In this paper, for the first time, a nonlinear thermo-electro-mechanical nonlinear couple formulation for piezo-flexoelectric functionally graded plate was extracted based on new reformulated flexoelectric theory, and then direct and inverse flexoelectric effects under different loadings were investigated. In order to indicate the contribution of the strain gradient tensor components, the reformulated flexoelectric theory [10] is applied in this paper. For this purpose, the strain gradient tensor is divided into independent part. Then, two set of higher order strain gradient tensor is employed to reformulated the internal energy density function for isotropic dielectrics.

2 PRELIMINARIES

The general form of internal energy density function for dielectric materials, which is a function of 36 homogeneous and quadratic variables as strain, strain gradient, polarization and its gradient, was introduced by Shen and Hu [52].

$$U = \frac{1}{2} C_{ijkl} \varepsilon_{ij} \varepsilon_{kl} + \frac{1}{2} g_{ijklmn} \eta_{ijk} \eta_{lmn} + \frac{1}{2} \alpha_{ij} P_i P_j + \frac{1}{2} b_{ijkl} Q_{ij} Q_{kl} + e_{ijk} Q_{ij} \varepsilon_{kl} + d_{ijk} \varepsilon_{ij} P_k + h_{ijk} P_i Q_{jk} + f_{ijkl} P_i \eta_{jkl} + r_{ijklm} \varepsilon_{ij} \eta_{klm} + s_{ijkmn} Q_{ij} \eta_{kmn} \quad (1)$$

where, e_{ijkl} and f_{ijkl} are the flexoelectric tensors with $e_{ijkl} = -f_{ijkl}$. This is due to the fact that Lifshitz invariant $f_{ijkl} (P_i \eta_{ijkl} - Q_{ij} \varepsilon_{kl})$ are relevant for the energy as was expressed by Eliseev, [53]. d_{ijkl} , g_{ijklmn} , b_{ijkl} represent the fourth-order piezoelectric coefficients tensor, pure nonlocal elastic effects and fourth order polarization gradient tensor, respectively. The constants s_{ijkmn} , r_{ijklm} , h_{ijk} are the other material property tensors and α_{ij} , C_{ijkl} are the second-order reciprocal dielectric susceptibility tensor and the fourth-order elastic constants tensor.

Using the derived internal energy density function, the constitutive equations are given by [52]:

$$\begin{aligned} \sigma_{ij} &= \frac{\partial U}{\partial \varepsilon_{ij}} = k \delta_{ij} \varepsilon_{nn} + 2\mu \varepsilon'_{ij} - f_1 \delta_{ij} Q_{kk} - 2f_2 Q_{ij}, \\ p_i &= \frac{\partial U}{\partial \gamma_i} = 2\mu l_0^2 \gamma_i + (f_1 + \frac{2}{3} f_2) P_i, \\ \tau_{ijk}^{(1)} &= \frac{\partial U}{\partial \eta_{ijk}^{(1)}} = 2\mu l_1^2 \eta_{ijk}^{(1)}, \\ m'_{ij} &= \frac{\partial U}{\partial \chi'_{ij}} = 2\mu (l_2^2 + \frac{9}{5} l_0^2) \chi'_{ij} + 2\mu (l_2^2 - \frac{9}{5} l_0^2) \chi'_{ji} + 2f_2 e_{ijk} P_k, \\ E_i &= \frac{\partial U}{\partial P_i} = \alpha P_i + (f_1 + \frac{2}{3} f_2) \gamma_i + 2f_2 e_{ijk} \chi'_{ji}, \\ V_{ij} &= \frac{\partial U}{\partial Q_{ij}} = \alpha (\delta_{ij} \beta_1^2 Q_{nn} + \beta_2^2 Q_{ji} + \beta_3^2 Q_{ji}) - f_{ij} \delta_{ij} \varepsilon_{nn} - 2f_2 \varepsilon_{ij}, \end{aligned} \quad (2)$$

where, the ε_{ij} , η_{ijk} , P_i , Q_{ij} , are strain tensor, strain gradients tensor, polarization vector and polarization gradient tensor, respectively.

Parameters l_i , β_i , respectively, are the length scale parameters related to the strain gradient, the length scale parameters related to the electric polarization gradient, and the quantities p_i , $\tau_{ijk}^{(1)}$ and m'_{ij} are the higher-order stress tensors. These tensors are related to dilatation gradient tensor γ_i , deviatoric stretch gradient tensor $\eta_{ijk}^{(1)}$ and deviatoric rotation gradient tensor χ'_{ij} , respectively [52].

The remaining material property tensors for isotropic dielectrics must be homogeneous linear functions of products of Kronecker delta, δ_{ij} . Thus, the dielectric tensor α_{ij} is taken to be constant, α , and the flexoelectric tensor f_{ijkl} is expressed as constants f_1, f_2 [10]. In addition, the moduli λ and μ are the Lamé constants for an isotropic material in Cauchy elasticity. Finally, the energy density function is written as [52]:

$$U = \frac{1}{2} \sigma_{ij} \varepsilon_{ij} + \frac{1}{2} \tau_{ijk}^{(1)} \eta_{ijk}^{(1)} + \frac{1}{2} p_i \gamma_i + \frac{1}{2} m'_{ij} \chi'_{ij} + \frac{1}{2} E_i P_i + \frac{1}{2} V_{ij} Q_{ij} \quad (3)$$

In this study, the effects of temperature rise are investigated. Thus, all constitutive equations in Eq. (2) will remain in the pervious form except the stress (σ_{ij}) and electric field (E_i) relations. These two relations were modified as follows [54]:

$$\sigma_{ij} = \frac{\partial U}{\partial \varepsilon_{ij}} = k \delta_{ij} \varepsilon_{nn} + 2\mu \varepsilon'_{ij} - f_1 \delta_{ij} Q_{kk} - 2f_2 Q_{ij} - \beta_{ij} \Delta T \quad (4)$$

$$E_i = \frac{\partial U}{\partial P_i} = \alpha P_i + (f_1 + \frac{2}{3} f_2) \gamma_i + 2f_2 e_{ijk} \chi'_{jk} - \gamma_i^T \Delta T \quad (5)$$

In the above equations, β_{ij} is the thermal modulus tensor given by:

$$\beta_{ij} = C_{ijkl} \alpha_{kl}^T \quad (6)$$

α_{kl}^T is the thermal expansion coefficients tensor. For an isotropic material:

$$\beta_{ij} = \alpha^T (3\lambda + 2\mu) \delta_{ij} \quad (7)$$

where $\alpha^T = \alpha_{33}^T$ is the thermal expansion coefficient and γ_i^T is a modified pyroelectric vector that $\gamma_i^T = \alpha_{ij}^{-1} \times \gamma_j$, [54]. Note that, γ_j is the pyroelectric vector.

3 GOVERNING EQUATIONS AND BOUNDARY CONDITIONS

In this study, the functionally graded flexoelectric nano-plate with thickness h , length a , and width b was modeled. The plate dimensions were assumed as $a=b=50*h$. Due to the functionally graded behavior of the nano-plate, the material properties vary along the plate thickness based on the power law model. According the classic Kirchhoff plate model, the displacement field is given by:

$$\begin{aligned} u(x, y, z) &= u_0(x, y) - z \frac{\partial w(x, y, z)}{\partial x} \\ v(x, y, z) &= v_0(x, y) - z \frac{\partial w(x, y, z)}{\partial y} \\ w(x, y, z) &= w(x, y) \end{aligned} \quad (8)$$

where u , v , and w are the each point displacements of the plate along the x -, y - and z -directions, respectively. $u_0(x, y)$ and $v_0(x, y)$ are the neutral plane displacement along the x and y directions, respectively.

In general, the displacement field is a function of the local and time coordinates, but in static analysis, this field is only a function of local coordinates. Regarding the displacement field, the strain-displacement relations are obtained as follows:

$$\begin{aligned} \varepsilon_{xx} &= \frac{\partial u}{\partial x} = \frac{\partial u_0}{\partial x} - z \frac{\partial^2 w}{\partial x^2} & \varepsilon_{xy} &= \frac{1}{2} \left(\frac{\partial u}{\partial x} + \frac{\partial v}{\partial x} \right) = \frac{1}{2} \left(\frac{\partial u_0}{\partial y} + \frac{\partial v_0}{\partial x} - 2z \frac{\partial^2 w}{\partial x \partial y} \right) \\ \varepsilon_{yy} &= \frac{\partial v}{\partial y} = \frac{\partial v_0}{\partial y} - z \frac{\partial^2 w}{\partial y^2} & \varepsilon_{xz} &= \frac{1}{2} \left(\frac{\partial u}{\partial z} + \frac{\partial w}{\partial x} \right) = \frac{1}{2} \left(-\frac{\partial w}{\partial x} + \frac{\partial w}{\partial x} \right) = 0 \\ \varepsilon_{zz} &= \frac{\partial w}{\partial z} = 0 & \varepsilon_{yz} &= \frac{1}{2} \left(\frac{\partial v}{\partial z} + \frac{\partial w}{\partial y} \right) = \frac{1}{2} \left(-\frac{\partial w}{\partial y} + \frac{\partial w}{\partial y} \right) = 0 \end{aligned} \quad (9)$$

In an electrostatic analysis, it is necessary to determine the electrical enthalpy energy density. This function is divided into the internal energy density and an additional part as suggested by Toupin [55].

$$H = U - \frac{1}{2} \varepsilon_0 \varphi_{,i} \varphi_{,i} + \varphi_{,i} P_i \quad (10)$$

In Eq. (10), ε_0 is the vacuum electrical permittivity constant, 8.854×10^{-12} (C/V.m), φ is the Electric Potential of the Maxwell electric field, P_i is the polarization vector in the nano-plate. Maxwell's electric field is determined via the following equation [10]:

$$E_i^{MS} = -\varphi_{,i} \quad (11)$$

The generalized electrostatic stress is also defined as follows [10]:

$$\begin{aligned} \sigma_{ij}^{ES} &= \sigma_{ki}^M - \tau_{kij,j}^M \\ \sigma_{ki}^M &= \frac{1}{2} E_j P_j \delta_{ij} - D_{ij} \varphi_{,k} + \left(-\frac{1}{2} \varepsilon_0 \varphi_{,j} \varphi_{,j} + \varphi_{,j} P_j \right) \delta_{ik} \\ \tau_{kij,j}^M &= V_{ij} P_{j,k} - \frac{1}{2} V_{lj} Q_{lj} \delta_{ik} \end{aligned} \quad (12)$$

D_i is the electrical displacement field, given by[10]:

$$D_i = -\varepsilon_0 \varphi_{,i} + P_i \quad (13)$$

Using the strain-displacement relations, the parameters in the constitutive equations and the total electrical enthalpy (Π_s) are obtained. The total electrical enthalpy is defined as follows [10]:

$$\Pi_s = \int_V H dV \quad (14)$$

The work done by the external classical forces is also defined as [21]:

$$\Pi_w = \int_0^b \int_0^a q w dx dy \quad (15)$$

In order to derive the governing equilibrium equations and related boundary conditions of the nano-plate, the variational method and the principle of minimum potential energy, are employed as [21]:

$$\delta \int_0^T (-\Pi_s + \Pi_w) = 0 \quad (16)$$

The principle of minimum potential energy is simplified by substituting the electric enthalpy density and the work done by the external forces, Eqs. (14) and (15) in Eq. (16), as follows:

$$-\delta \int_V H dV + \int_A q \delta w dA = 0 \quad (17)$$

According to Reynolds transport theory, $\delta \int_V H dV$ is written as follows[10]:

$$\delta \int_V H dV = \int_V \delta H dV + \int_V H \delta u_{k,k} dV \quad (18)$$

Substituting the enthalpy energy (Eq. (10)) in Eq. (18), the above expression is simplified to be:

$$\delta \int_V H dV = \int_V \delta U dV + \int_V \delta \left(-\frac{1}{2} \varepsilon_0 \varphi_{,i} \varphi_{,i} + \varphi_{,i} P_i \right) dV + \int_V U \delta u_{k,k} dV + \int_V \left(-\frac{1}{2} \varepsilon_0 \varphi_{,i} \varphi_{,i} + \varphi_{,i} P_i \right) \delta u_{k,k} dV \quad (19)$$

Substituting the strain components Eq. (9) in Eq. (1), the internal energy density, which contains 47 components, is obtained. Finally, using the variation method and direct mathematical simplifications, the integral $\delta \int_V U dV$ is evaluated. The upper and lower surfaces of functionally graded piezo-flexoelectric nano-plate are made of PZT-4 and PZT-5H, respectively (Fig. 1).

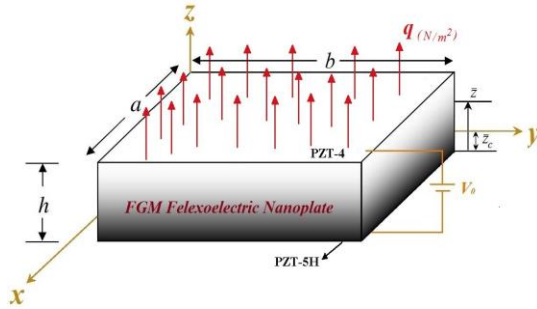


Fig.1
Schematic of functionally graded flexoelectric nano-plate.

In this figure:

$$z = \bar{z} - \bar{z}_c \quad (20)$$

\bar{z}_c is the distance of the neutral plane to the bottom surface and \bar{z} is the distance between any arbitrary layer measured from the bottom surface.

It should be noted that the initial created strain in one of the middle surfaces of the nano-plate will be zero due to the bending axial stress [56]. Thus, the neutral plane position is determined from:

$$\int_A \sigma_{11}^0 dA = 0 \quad (21)$$

Substituting the stress in Eq. (21), the distance of neutral plane to the lower surface is [47]:

$$\bar{z}_c = \frac{\int_A \frac{E(z)}{1-\nu^2(z)} z dA}{\int_A \frac{E(z)}{1-\nu^2(z)} dA} \quad (22)$$

The functionally graded behavior of the nano-plate is modeled using a power law equation. Thus, the nano-plate properties such as elastic constants ($E(z)$, $\nu(z)$, $\lambda(z)$, $\mu(z)$), electrical properties (piezoelectric coefficients, flexoelectric coefficients, dielectric constants) and thermal properties (thermal expansion constant, pyroelectric coefficients, thermal modulus) are defined in the following form.

$$M(z) = M_1 + (M_2 - M_1) \left(\frac{z + \bar{z}_c}{h} \right)^n, \quad (23)$$

where, M_1 and M_2 are the material properties corresponding to the lower and the upper plate surfaces, respectively. In addition, n is the power index of the functionally graded model. Finally, $M(z)$ is the desired quantity of the FGM nano-plate along the thickness direction.

The equilibrium equations and boundary conditions are obtained by substituting Eqs. (2) and (3) in Eq. (19) and using the principle of minimum potential energy (Eq. (17)). The resulting relations are:

$$-\frac{\partial(N_{xx})}{\partial x} - \frac{\partial Q}{\partial x} + \frac{\partial^2(N_{xx}^{hx})}{\partial x^2} + \frac{\partial^2(N_{yy}^{hx})}{\partial y^2} + \frac{\partial^2(N_{xy}^{hx})}{\partial x \partial y} = 0 \quad (24)$$

$$-\frac{\partial(N_{yy})}{\partial y} - \frac{\partial Q}{\partial y} + \frac{\partial^2(N_{xx}^{hy})}{\partial x^2} + \frac{\partial^2(N_{yy}^{hy})}{\partial y^2} + \frac{\partial^2(N_{xy}^{hy})}{\partial x \partial y} = 0 \quad (25)$$

$$\frac{\partial^2(M_{xx})}{\partial x^2} - \frac{\partial^2(M_{yy})}{\partial y^2} - \frac{\partial^2(M_{xy})}{\partial x \partial y} - \frac{\partial^3(M_{xx}^h)}{\partial x^3} - \frac{\partial^3(M_{yy}^h)}{\partial y^3} - \frac{\partial^3(M_{xxy}^h)}{\partial x^2 \partial y} - \frac{\partial^3(M_{xyy}^h)}{\partial x \partial y^2} + q = 0 \quad (26)$$

$$E_3 - \frac{\partial(V_{33})}{\partial z} - \frac{\partial \phi}{\partial z} = 0 \quad (27)$$

$$-\frac{\partial D_3}{\partial z} = \varepsilon_o \phi_{3,3} + P_{3,3} = 0 \quad (28)$$

The boundary conditions are determined to be:

$$\begin{aligned} \left[-N_{xx} + \frac{\partial(N_{xx}^{hx})}{\partial x} \right]_{x=0,a} &= 0 & \text{or } \delta u_0|_{x=0,a} &= 0 \\ \left[-Q + \frac{\partial(N_{xy}^{hx})}{\partial x} + \frac{\partial(N_{yy}^{hx})}{\partial y} \right]_{y=0,b} &= 0 & \text{or } \delta u_0|_{y=0,b} &= 0 \\ \left[-N_{xx}^{hx} \right]_{x=0,a} &= 0 & \text{or } \frac{d(\delta u_0)}{dx} \Big|_{x=0,a} &= 0 \\ \left[-N_{xy}^{hx} \right]_{x=0,a} &= 0 & \text{or } \frac{d(\delta u_0)}{dy} \Big|_{x=0,a} &= 0 \\ \left[-N_{yy}^{hx} \right]_{y=0,b} &= 0 & \text{or } \frac{d(\delta u_0)}{dy} \Big|_{y=0,b} &= 0 \end{aligned} \quad (29)$$

$$\begin{aligned} \left[-Q + N_{xy}^{hy} \right]_{x=0,a} &= 0 & \text{or } \delta v_0|_{x=0,a} &= 0 \\ \left[-N_{yy} + \frac{\partial(N_{xy}^{hy})}{\partial x} + \frac{\partial(N_{yy}^{hy})}{\partial y} \right]_{y=0,b} &= 0 & \text{or } \delta v_0|_{y=0,b} &= 0 \\ \left[-N_{xx}^{hy} \right]_{x=0,a} &= 0 & \text{or } \frac{d(\delta v_0)}{dx} \Big|_{x=0,a} &= 0 \\ \left[-N_{xy}^{hy} \right]_{x=0,a} &= 0 & \text{or } \frac{d(\delta v_0)}{dy} \Big|_{x=0,a} &= 0 \\ \left[-N_{yy}^{hy} \right]_{y=0,b} &= 0 & \text{or } \frac{d(\delta v_0)}{dy} \Big|_{y=0,b} &= 0 \end{aligned} \quad (30)$$

$$\begin{aligned}
\left[\frac{\partial(M_{xx})}{\partial x} + \frac{\partial^2(M_{xx}^h)}{\partial x^2} \right]_{x=0,a} &= 0 & \text{or } \delta w|_{x=0,a} &= 0 \\
\left[\frac{\partial(M_{xy})}{\partial x} + \frac{\partial(M_{yy})}{\partial y} + \frac{\partial^2(M_{xxy})}{\partial x^2} + \frac{\partial^2(M_{yy}^h)}{\partial y^2} + \frac{\partial^2(M_{xyy})}{\partial x \partial y} \right]_{y=0,b} &= 0 & \text{or } \delta w|_{y=0,b} &= 0 \\
\left[-M_{xx} - \frac{\partial(M_{xx}^h)}{\partial x} \right]_{x=0,a} &= 0 & \text{or } \frac{d(\delta w)}{dx} \Big|_{x=0,a} &= 0 \\
\left[-M_{xy} - \frac{\partial(M_{xxy}^h)}{\partial x} - \frac{\partial(M_{xyy}^h)}{\partial y} \right]_{x=0,a} &= 0 & \text{or } \frac{d(\delta w)}{dy} \Big|_{x=0,a} &= 0 \\
\left[M_{yy} - \frac{\partial(M_{xyy}^h)}{\partial x} - \frac{\partial(M_{yy}^h)}{\partial y} \right]_{y=0,b} &= 0 & \text{or } \frac{d(\delta w)}{dy} \Big|_{y=0,b} &= 0 \\
\left[-M_{xx}^h \right]_{x=0,a} &= 0 & \text{or } \frac{d^2(\delta w)}{dx^2} \Big|_{x=0,a} &= 0 \\
\left[-M_{yy}^h \right]_{y=0,b} &= 0 & \text{or } \frac{d^2(\delta w)}{dy^2} \Big|_{y=0,b} &= 0 \\
\left[-M_{xxy}^h - M_{xyy}^h \right]_{x=0,a} &= 0 & \text{or } \frac{d^2(\delta w)}{dxdy} \Big|_{x=0,a} &= 0
\end{aligned} \tag{31}$$

and the electrical boundary conditions are as follows:

$$\begin{aligned}
@z = -z_c, h - z_c \quad V_{33} &= 0 & \text{or } (\delta P_3)_{-z_c}^{h-z_c} &= 0 \\
@z = -z_c, h - z_c \quad D_3 &= 0 & \text{or } (\delta \varphi)_{-z_c}^{h-z_c} &= 0
\end{aligned} \tag{32}$$

Applying the variational principle on the integral $\int_V HdV$, the expressions for the resultants first and higher order stress and moment in Eqs. (24) to (26) are found to be:

$$\begin{aligned}
N_{xx} &= N_{11} + N_{11}^{ES} = \int_{-z_c}^{h-z_c} (\sigma_{11} + \sigma_{11}^{ES}) dz \\
Q &= N_{\sigma_{12}} = \int_{-z_c}^{h-z_c} \sigma_{12} dz \\
N_{xx}^{hx} &= N_{p_1} + \frac{1}{3} N_{m'23} - \frac{1}{3} N_{m'32} - \frac{3}{5} N_{\tau_{122}}^{(1)} + \frac{7}{10} N_{\tau_{111}}^{(1)} \\
N_{yy}^{hx} &= N_{\tau_{212}}^{(1)} - \frac{1}{2} N_{m'32} \\
N_{xy}^{hx} &= N_{p_2} - \frac{1}{3} N_{m'13} - \frac{1}{3} N_{m'31} - \frac{34}{5} N_{\tau_{233}}^{(1)} - \frac{2}{5} N_{\tau_{222}}^{(1)}
\end{aligned} \tag{33}$$

$$N_{yy} = N_{\sigma_{22}} = \int_{-z_c}^{h-z_c} \sigma_{22} dz$$

$$N_{xx}^h = \frac{1}{6} N_{m'_{32}} - \frac{1}{2} N_{m'_{31}} - \frac{7}{12} N_{\tau_{233}}^{(1)} - \frac{1}{5} N_{\tau_{222}}^{(1)} \quad (34)$$

$$N_{yy}^h = N_{p_2} - \frac{1}{3} N_{m'_{13}} + \frac{1}{3} N_{m'_{31}} - \frac{1}{5} N_{\tau_{222}}^{(1)}$$

$$M_{xx} = -N_{p_3} - \frac{1}{3} N_{m'_{12}} - \frac{2}{3} N_{m'_{21}} - \frac{19}{20} N_{\tau_{113}}^{(1)} + \frac{1}{5} N_{\tau_{223}}^{(1)} + M_{\sigma_{11}} - M_{\sigma_{11}^{Es}}$$

$$M_{yy} = -N_{p_3} - \frac{2}{3} N_{m'_{12}} - \frac{1}{3} N_{m'_{21}} - N_{\tau_{223}}^{(1)} - M_{\sigma_{22}}$$

$$M_{xy} = -N_{m'_{11}} - \frac{2}{3} N_{m'_{22}} - 2N_{\tau_{123}}^{(1)} - 2M_{\sigma_{12}}$$

$$M_{xx}^h = M_{p_1} + \frac{1}{3} M_{m'_{23}} - \frac{1}{3} M_{m'_{32}} - \frac{7}{5} M_{\tau_{133}}^{(1)} + \frac{3}{5} N_{\tau_{212}}^{(1)} + \frac{4}{5} M_{\tau_{211}}^{(1)} \quad (35)$$

$$M_{yy}^h = M_{p_2} - \frac{1}{3} M_{m'_{13}} + \frac{1}{3} M_{m'_{31}} + M_{\tau_{222}}^{(1)}$$

$$M_{xxy}^h = M_{p_2} - \frac{1}{3} M_{m'_{13}} + \frac{1}{3} M_{m'_{31}} + \frac{1}{3} M_{m'_{23}} - 7M_{\tau_{223}}^{(1)} - \frac{3}{5} M_{\tau_{222}}^{(1)}$$

$$M_{xxy}^h = M_{p_1} - \frac{1}{3} M_{m'_{32}} + 3M_{\tau_{212}}^{(1)} + \frac{1}{3} M_{m'_{23}}$$

N_f and M_f in the right hand side expressions in Eqs. (33) to (35), are defined as follows.

$$N_f = \int_{-z_c}^{h-z_c} f dz \quad M_f = \int_{-z_c}^{h-z_c} z \times f dz \quad (36)$$

where, f can be a vector (f_i), a second-order tensor (f_{ij}), or a third-order tensor (f_{ijk}).

Also, the terms $M_{ij}^h, M_{ij}, N_{ij}^h, Q, N_{ij}$ on the left hand side of the Eqs. (33) to (35), are respectively the axial stress resultant, the shear stress resultant, the higher-order axial stress resultant, the moment resultant, and the higher-order moment resultant. Using the constitutive Eqs. (2) and (13), the electrical equilibrium equations are simplified as follows:

$$\alpha P_3(z) - 2f_1 \nabla^2 w - \gamma^T(z) \Delta T(z) - \alpha \beta^2 \frac{\partial^2 P_3(z)}{\partial z^2} + \frac{\partial \varphi(z)}{\partial z} = 0 \quad (37)$$

$$\varepsilon_o \frac{\partial^2 \varphi(z)}{\partial z^2} - \frac{\partial P_3(z)}{\partial z} = 0 \quad (38)$$

where $\beta^2 = \sqrt{\beta_1^2 + \beta_2^2 + \beta_3^2}$, [10]. It should be noted that the temperature variation along the plate thickness is assumed linear, as given by;

$$\Delta T(z) = (T_2 - T_1) \left(\frac{1}{2} + \frac{z}{h} \right) \quad (39)$$

Due to the power law model of FGM nano-plate, the modified pyroelectric coefficient $\gamma^T(z)$ is defined as follows;

$$\gamma^T(z) = \gamma_1^T + (\gamma_2^T - \gamma_1^T) \left(\frac{1}{2} + \frac{z}{h} \right)^n \quad (40)$$

4 BENDING SOLUTION OF FLEXOELECTRIC NANO-PLATE

4.1 Direct flexoelectric effect

In this section, the governing equations of functionally graded nano-plate subjected to a distributed mechanical loading are obtained in terms of the nano-plate displacement field components. Using the boundary conditions (32) and $\varphi(-z_c)=0$, [10], the system of differential Eqs. (27) and (28) are solved to determine the polarization, $P_3(z)$, and electrical potential, $\varphi(z)$, as follows:

$$P_3(z) = A1 + (A2)e^{g.z} + (A3)e^{-g.z} - \frac{R.z}{g^2} \quad (41)$$

$$\varphi(z) = \frac{1}{g.\varepsilon_0} \left[(A2)e^{g.z} - (A3)e^{-g.z} - \frac{R.z}{g^2} \right] + (B1)Z + B2 \quad (42)$$

where:

$$A1 = \frac{4f_{1a} \times \varepsilon_0 \left(\frac{\partial^2 w(x,y)}{\partial x^2} + \frac{\partial^2 w(x,y)}{\partial y^2} \right) + \gamma_a^T \times \varepsilon_0 (T2 - T1)}{2(1 + \alpha_a \times \varepsilon_0)} \quad (43)$$

$$A2 = -\frac{g \times \varepsilon_0}{1 + \alpha_a \times \varepsilon_0} (S_1 \times f_{1h} + S_2 \times f_{2h})$$

$$A3 = -\frac{g \times \varepsilon_0}{1 + \alpha_a \times \varepsilon_0} (S_1 \times f_{3h} + S_2 \times f_{4h})$$

$$S_1 = f_{1a} \left[\frac{\partial^2 u_0(x,y)}{\partial x} + \frac{\partial^2 v_0(x,y)}{\partial y} + zc \left(\frac{\partial^2 w(x,y)}{\partial x^2} + \frac{\partial^2 w(x,y)}{\partial y^2} \right) \right] + \frac{\alpha_a \times \beta^2 \times R}{g^2} \quad (44)$$

$$S_2 = f_{1a} \times h \left(\frac{\partial^2 w(x,y)}{\partial x^2} + \frac{\partial^2 w(x,y)}{\partial y^2} \right)$$

$$f_{1h} = \frac{e^{-g.h}}{e^{g.h} - e^{-g.h}}, f_{2h} = \frac{e^{-g.z_c}}{e^{g.h} - e^{-g.h}}, f_{3h} = \frac{e^{g.h}}{e^{g.h} - e^{-g.h}}, f_{4h} = \frac{e^{-g.z_c}}{e^{g.h} - e^{-g.h}}, \quad (45)$$

$$\alpha_a = \frac{1}{h} \int_{-z_c}^{h-z_c} \left[\alpha_1 + (\alpha_2 - \alpha_1) \left(\frac{1}{2} + \frac{z}{h} \right)^n \right] dz,$$

$$f_{1a} = \frac{1}{h} \int_{-z_c}^{h-z_c} \left[f_{11} + (f_{12} - f_{11}) \left(\frac{1}{2} + \frac{z}{h} \right)^n \right] dz \quad (46)$$

$$\gamma_a^T = \frac{1}{h} \int_{-z_c}^{h-z_c} \left[\gamma_1^T + (\gamma_2^T - \gamma_1^T) \left(\frac{1}{2} + \frac{z}{h} \right)^n \right] dz, \quad g^2 = \frac{1 + \alpha_a \varepsilon_0}{\alpha_a \varepsilon \beta^2}$$

$$R = \frac{\gamma_a^T (T_2 - T_1)}{\alpha_a \times \beta^2 \times h} \tag{47}$$

$$B1 = \frac{A_1}{\varepsilon_0}, \quad B2 = B1 \times z_c - \frac{1}{g \times \varepsilon_0} \left[(A2)e^{-g z_c} - (A3)e^{g z_c} - \frac{R \times z_c^2}{2g} \right]$$

The constants $\gamma_a^T, f_{1a}, \alpha_a$ are the FG nano-plate modified pyroelectric coefficient, flexoelectric coefficient, f_i , and reciprocal dielectric susceptibility coefficient along the plate thickness, respectively. Also, the constants α_1, α_2 are dielectric coefficients, f_{11}, f_{12} are the flexoelectric coefficients and γ_1^T, γ_2^T are the modified pyroelectric coefficients for the bottom and upper nano-plate surfaces, respectively.

The parameters in Eq. (2) are determined by employing the Eqs. (41, 42) and strain–displacement relation. Substituting these parameters in Eqs. (33) to (35), the terms in Eqs. (24) to (26) are obtained in terms of displacement field of the functionally graded nano-plate. The resulting relations are:

$$N_{xx} = A_1 \left(\frac{\partial^2 w}{\partial x^2} \right)^2 + A_2 \left(\frac{\partial^2 w}{\partial y^2} \right)^2 + A_3 \left(\frac{\partial u_o}{\partial x} \right)^2 + A_4 \left(\frac{\partial v_o}{\partial y} \right)^2 + A_5 + A_6 \left(\frac{\partial^2 w}{\partial x^2} \right)$$

$$+ A_7 \left(\frac{\partial u_o}{\partial x} \frac{\partial^2 w}{\partial x^2} \right) + A_8 \left(\frac{\partial v_o}{\partial y} \frac{\partial^2 w}{\partial x^2} \right) + A_9 \left(\frac{\partial^2 w}{\partial y^2} \frac{\partial^2 w}{\partial x^2} \right) + A_{10} \left(\frac{\partial^2 w}{\partial x^2} \right) + A_{11} \left(\frac{\partial u_o}{\partial x} \frac{\partial^2 w}{\partial y^2} \right)$$

$$+ A_{12} \left(\frac{\partial v_o}{\partial y} \frac{\partial^2 w}{\partial y^2} \right) + A_{13} \left(\frac{\partial u_o}{\partial x} \right) + A_{14} \left(\frac{\partial u_o}{\partial x} \frac{\partial v_o}{\partial y} \right) + A_{15} \left(\frac{\partial v_o}{\partial y} \right)$$

$$N_{xx}^{hx} = B_1 \left(\frac{\partial^3 w}{\partial x^3} \right) + B_2 \left(\frac{\partial^3 w}{\partial x \partial y^2} \right) + B_{31} \left(\frac{\partial^2 u_o}{\partial x^2} \right) + B_4 \left(\frac{\partial^2 u_o}{\partial y^2} \right) + B_5 \left(\frac{\partial^2 v_o}{\partial x \partial y} \right) \tag{48}$$

$$N_{yy}^{hx} = C_1 \left(\frac{\partial^3 w}{\partial x^3} \right) + C_2 \left(\frac{\partial^3 w}{\partial x \partial y^2} \right) + C_3 \left(\frac{\partial^2 u_o}{\partial x^2} \right) + C_4 \left(\frac{\partial^2 u_o}{\partial y^2} \right) + C_5 \left(\frac{\partial^2 v_o}{\partial x \partial y} \right)$$

$$N_{xy}^{hx} = D_1 \left(\frac{\partial^3 w}{\partial x^3} \right) + D_2 \left(\frac{\partial^3 w}{\partial x \partial y^2} \right) + D_3 \left(\frac{\partial^2 u_o}{\partial x \partial y} \right) + D_4 \left(\frac{\partial^2 v_o}{\partial x^2} \right) + D_5 \left(\frac{\partial^2 v_o}{\partial y^2} \right)$$

$$Q = EQ \left(\frac{\partial^2 w}{\partial x \partial y} \right)_1 + EQ_2 \left(\frac{\partial u_o}{\partial y} \right) + EQ_3 \left(\frac{\partial v_o}{\partial x} \right)$$

$$N_{yy} = F_1 \left(\frac{\partial^2 w}{\partial x^2} \right) + F_2 \left(\frac{\partial^2 w}{\partial y^2} \right) + F_3 \left(\frac{\partial u_o}{\partial x} \right) + F_4 \left(\frac{\partial v_o}{\partial y} \right) + F_5$$

$$N_{xx}^{hy} = G_1 \left(\frac{\partial^3 w}{\partial x^3} \right) + G_2 \left(\frac{\partial^3 w}{\partial y^3} \right) + G_3 \left(\frac{\partial^3 w}{\partial x \partial y^2} \right) + G_4 \left(\frac{\partial^3 w}{\partial y \partial x^2} \right) + G_5 \left(\frac{\partial^2 u_o}{\partial x^2} \right)$$

$$+ G_6 \left(\frac{\partial^2 u_o}{\partial y^2} \right) + G_7 \left(\frac{\partial^2 u_o}{\partial x \partial y} \right) + G_8 \left(\frac{\partial^2 v_o}{\partial x^2} \right) + G_9 \left(\frac{\partial^2 v_o}{\partial y^2} \right) + G_{10} \left(\frac{\partial^2 v_o}{\partial x \partial y} \right) \tag{49}$$

$$N_{yy}^{hy} = H_1 \left(\frac{\partial^3 w}{\partial y^3} \right) + H_2 \left(\frac{\partial^3 w}{\partial y \partial x^2} \right) + H_3 \left(\frac{\partial^2 u_o}{\partial x \partial y} \right) + H_4 \left(\frac{\partial^2 v_o}{\partial x^2} \right) + H_5 \left(\frac{\partial^2 v_o}{\partial y^2} \right)$$

$$N_{xy}^{hy} = I_1 \left(\frac{\partial^3 w}{\partial x^3} \right) + I_2 \left(\frac{\partial^3 w}{\partial x \partial y^2} \right) + I_3 \left(\frac{\partial^2 u_o}{\partial x^2} \right) + I_4 \left(\frac{\partial^2 u_o}{\partial y^2} \right) + I_5 \left(\frac{\partial^2 v_o}{\partial x \partial y} \right)$$

$$\begin{aligned}
M_{xx} &= J_1 \left(\frac{\partial^2 w}{\partial x^2} \right)^2 + J_2 \left(\frac{\partial^2 w}{\partial y^2} \right)^2 + J_3 \left(\frac{\partial u_o}{\partial x} \right)^2 + J_4 \left(\frac{\partial v_o}{\partial y} \right)^2 + J_5 + J_6 \left(\frac{\partial^2 w}{\partial x^2} \right) + J_7 \left(\frac{\partial^2 w}{\partial x^2} \frac{\partial^2 w}{\partial y^2} \right) + J_8 \left(\frac{\partial^2 w}{\partial x^2} \frac{\partial u_o}{\partial x} \right) \\
&+ J_9 \left(\frac{\partial^2 w}{\partial x^2} \frac{\partial v_o}{\partial y} \right) + J_{10} \left(\frac{\partial^2 w}{\partial y^2} \right) + J_{11} \left(\frac{\partial^2 w}{\partial y^2} \frac{\partial u_o}{\partial x} \right) + J_{12} \left(\frac{\partial^2 w}{\partial y^2} \frac{\partial v_o}{\partial y} \right) + J_{13} \left(\frac{\partial u_o}{\partial x} \right) + J_{14} \left(\frac{\partial v_o}{\partial y} \frac{\partial u_o}{\partial x} \right) + J_{15} \left(\frac{\partial v_o}{\partial y} \right) + J_{16} \left(\frac{\partial^3 w}{\partial x \partial y^2} \right) \\
M_{yy} &= K_1 \frac{\partial^2 w}{\partial x^2} + K_2 \frac{\partial^2 w}{\partial y^2} + K_3 \frac{\partial^3 u_o}{\partial x \partial y^2} + K_4 \frac{\partial u_o}{\partial x} + k_5 \frac{\partial v_o}{\partial y} + k_6 \\
M_{xy} &= L_1 \frac{\partial^2 w}{\partial x \partial y} + L_2 \frac{\partial u_o}{\partial y} + L_3 \frac{\partial v_o}{\partial x} \\
M_{xx}^h &= M_1 \frac{\partial^3 w}{\partial x^3} + M_2 \frac{\partial^3 w}{\partial x \partial y} + M_3 \frac{\partial^3 w}{\partial y \partial x^2} + M_4 \frac{\partial^2 u_o}{\partial x^2} + M_5 \frac{\partial^2 u_o}{\partial y^2} + M_6 \frac{\partial^2 u_o}{\partial x \partial y} + M_7 \frac{\partial^2 v_o}{\partial x^2} + M_8 \frac{\partial^2 v_o}{\partial x \partial y} \\
M_{yy}^h &= N_1 \frac{\partial^3 w}{\partial y^3} + N_2 \frac{\partial^3 w}{\partial y \partial x^2} + N_3 \frac{\partial^2 u_o}{\partial x \partial y} + N_4 \frac{\partial^2 v_o}{\partial x^2} + N_5 \frac{\partial^2 v_o}{\partial y^2} \\
M_{xxy}^h &= P_1 \frac{\partial^3 w}{\partial x^3} + P_2 \frac{\partial^3 w}{\partial y^3} + P_3 \frac{\partial^2 w}{\partial x \partial y^2} + P_4 \frac{\partial^3 w}{\partial y \partial x^2} + P_5 \frac{\partial^2 u_o}{\partial x^2} + P_6 \frac{\partial^2 u_o}{\partial y^2} + P_7 \frac{\partial^2 u_o}{\partial x \partial y} + P_8 \frac{\partial^2 v_o}{\partial x^2} + P_9 \frac{\partial^2 v_o}{\partial y^2} + P_{10} \frac{\partial^2 v_o}{\partial x \partial y} \\
M_{xyy}^h &= Q_1 \frac{\partial^3 w}{\partial x^3} + Q_2 \frac{\partial^3 w}{\partial x \partial y^2} + Q_3 \frac{\partial^2 u_o}{\partial x^2} + Q_4 \frac{\partial^2 u_o}{\partial y^2} + Q_5 \frac{\partial^2 v_o}{\partial x \partial y}
\end{aligned} \tag{50}$$

The constants A_i , B_i , C_i , D_i , E , Q_i , F_i , G_i , H_i , I_i , J_i , K_i , L_i , M_i , N_i , P_i and Q_i are material derivative that are calculated by integration of the respective parameters along the z -direction.

Sinusoidal displacement field components are considered in the following form [44]:

$$\begin{aligned}
u_o(x, y) &= A \cos \frac{\pi x}{a} \sin \frac{\pi y}{b} \\
v_o(x, y) &= B \sin \frac{\pi x}{a} \cos \frac{\pi y}{b} \\
w(x, y) &= C \sin \frac{\pi x}{a} \sin \frac{\pi y}{b}
\end{aligned} \tag{51}$$

The above displacement fields satisfy all of the nano-plate boundary conditions with four simply supported edges. Using the Galerkin's method, the mentioned mechanical equilibrium equations are simplified into system of the non-linear algebraic equations in terms of the displacement field and constants in Eqs. (48-50). for this plate, the relevant Boundary conditions are given by [44]:

$$\begin{aligned}
v = w = \frac{\partial^2 w}{\partial x^2} = 0 \quad @x = 0, a \\
u = w = \frac{\partial^2 w}{\partial y^2} = 0 \quad @y = 0, b
\end{aligned} \tag{52}$$

Once the constants A , B , C , are determined. Also, the displacement field of the functionally graded nano-plate is obtained. Afterwards, the polarization functions and electric potential are extracted.

Substituting Eqs. (48) through (50) in equilibrium equations, these equations are written in terms of displacement field components as follows:

$$\begin{aligned}
 &-(C_1+D_2+B_2)\frac{\partial^5 w(x,y)}{\partial y^2 \partial x^3}-(C_2+D_1)\frac{\partial^5 w(x,y)}{\partial y^4 \partial x}-(+B_1)\frac{\partial^5 w(x,y)}{\partial x^5}-(C_3+D_3+B_4)\frac{\partial^4 u_0(x,y)}{\partial y^2 \partial x^2}-(D_4+B_5)\frac{\partial^4 v_0(x,y)}{\partial y \partial x^3} \\
 &-(C_5+D_5)\frac{\partial^4 v_0(x,y)}{\partial y^3 \partial x}-(B_3)\frac{\partial^4 u_0(x,y)}{\partial x^4}-(C_4)\frac{\partial^4 u_0(x,y)}{\partial y^4}+(EQ_1)\frac{\partial^3 w(x,y)}{\partial y \partial x^2}+(EQ_2)\frac{\partial^2 u_0(x,y)}{\partial y \partial x}+(EQ_3)\frac{\partial^2 v_0(x,y)}{\partial x^2} \\
 &+\left[(A_9)\frac{\partial v_0(x,y)}{\partial y}+(2A_1)\frac{\partial^4 w(x,y)}{\partial x^2}+(A_8)\frac{\partial u_0(x,y)}{\partial x}+(A_7)\frac{\partial^2 w(x,y)}{\partial y^2}+(A_6)\right]\frac{\partial^3 w(x,y)}{\partial x^3} \\
 &+\left[(A_{11})\frac{\partial u_0(x,y)}{\partial x}+(A_{12})\frac{\partial v_0(x,y)}{\partial y}+(2A_2)\frac{\partial^2 w(x,y)}{\partial y^2}+(A_7)\frac{\partial^2 w(x,y)}{\partial x^2}+(A_{10})\right]\frac{\partial^3 w(x,y)}{\partial y^2 \partial x}+\left[(A_{11})\frac{\partial^2 w(x,y)}{\partial y^2}\right. \\
 &+\left.(A_{14})\frac{\partial v_0(x,y)}{\partial y}+(2A_3)\frac{\partial u_0(x,y)}{\partial x}+(A_8)\frac{\partial^2 w(x,y)}{\partial x^2}+(A_{13})\right]\frac{\partial^2 u_0(x,y)}{\partial x^2}+ \\
 &\left[(A_9)\frac{\partial^2 w(x,y)}{\partial x^2}+(A_{12})\frac{\partial^2 w(x,y)}{\partial y^2}+(A_{14})\frac{\partial u_0(x,y)}{\partial x}+(2A_4)\frac{\partial v_0(x,y)}{\partial y}+(A_{15})\right]\frac{\partial^2 u_0(x,y)}{\partial x^2}=0
 \end{aligned} \tag{53}$$

$$\begin{aligned}
 &-(G_2+H_2+I_2)\frac{\partial^5 w(x,y)}{\partial y^3 \partial x^2}-(G_4+I_1)\frac{\partial^5 w(x,y)}{\partial y \partial x^4}-(G_1)\frac{\partial^5 w(x,y)}{\partial x^5}-(G_3)\frac{\partial^5 w(x,y)}{\partial y^2 \partial x^3}-(H_1)\frac{\partial^5 w(x,y)}{\partial y^5} \\
 &-(G_9+H_4+I_5)\frac{\partial^4 v_0(x,y)}{\partial y^2 \partial x^2}-(G_7+I_3)\frac{\partial^4 u_0(x,y)}{\partial y \partial x^3}-(H_3+I_4)\frac{\partial^4 u_0(x,y)}{\partial y^3 \partial x}-(G_5)\frac{\partial^4 u_0(x,y)}{\partial x^4} \\
 &-(G_6)\frac{\partial^4 u_0(x,y)}{\partial y^2 \partial x^2}-(G_8)\frac{\partial^4 v_0(x,y)}{\partial x^4}-(G_{10})\frac{\partial^4 v_0(x,y)}{\partial y \partial x^3}-(H_5)\frac{\partial^4 v_0(x,y)}{\partial y^4}+(F_1)\frac{\partial^3 w(x,y)}{\partial y \partial x^2} \\
 &+(F_2)\frac{\partial^3 w(x,y)}{\partial y^3}+(F_3)\frac{\partial^2 u_0(x,y)}{\partial y \partial x}+(F_4)\frac{\partial^2 v_0(x,y)}{\partial y^2}=0
 \end{aligned} \tag{54}$$

4.2 Inverse flexoelectric effect

In this section, the displacement field, the electrical polarization function and the electrical potential of the nano-plate are determined for the plate subjected to a distributed mechanical loading q and an external applied voltage V_0 along the plate thickness direction. With the boundary conditions related to mentioned applied loadings, the system of differential Eqs. (27) and (28) were solved, and the functions of electric polarization $P_3(z)$ and electrical potential $\varphi(z)$ are determined.

The electrical boundary conditions of nano-plate under the external applied voltage along the thickness direction are as follows [10].

$$\begin{aligned}
 @z = -z_c, h - z_c & \quad V_{33} = 0 \\
 @z = h - z_c & \quad \varphi(h - z_c) = V_0 \\
 @z = -z_c & \quad \varphi(-z_c) = 0
 \end{aligned} \tag{55}$$

The functions $P_3(z)$ and $\varphi(z)$ are obtained by solving the system of Eqs. (56) and (57) and the new boundary conditions. The resulting relations are:

$$P_3(z) = A1 + (A2)e^{g.z} + (A3)e^{-g.z} - \frac{R.z}{g^2} \tag{56}$$

$$\varphi(z) = \frac{1}{g.\epsilon_0} \left[(A2)e^{g.z} - (A3)e^{-g.z} - \frac{R.z}{g^2} \right] + (B1)Z + B2 \tag{57}$$

where:

$$\begin{aligned}
A1 &= \frac{1}{g \times \alpha_a \times \varepsilon_0 \times h} \left[(A2)(e^{g.h} - 1)e^{-g.z_c} - (A3)(e^{-g.h} - 1)e^{g.z_c} - \frac{R.(h^2 - 2h \times z_c)}{2g} \right] \\
&\quad - \frac{V_0}{\alpha_a \times h} - \frac{2f_{1a}}{\alpha_a} \left(\frac{\partial^2 w(x, y)}{\partial x^2} + \frac{\partial^2 w(x, y)}{\partial y^2} \right) \\
B1 &= \frac{1}{g \times \varepsilon_0 \times h} \left[(A2)(e^{g.h} - 1)e^{-g.z_c} - (A3)(e^{-g.h} - 1)e^{g.z_c} - \frac{R.(h^2 - 2h \times z_c)}{2g} \right] + \frac{V_0}{h}, \\
B2 &= B1 \times z_c - \frac{1}{g \times \varepsilon_0} \left[(A2)e^{-g.z_c} - (A3)e^{g.z_c} - \frac{R.z_c^2}{2g} \right]
\end{aligned} \tag{58}$$

Note that the other coefficients are the same as the ones presented in the previous section. Substituting Eqs. (56) and (57) in Eqs. (33) to (35) and applying Eqs. (48) through (50), the equilibrium equations are determined in terms of the displacement field of the nano-plate. The results of these analyses are presented in the following sections.

5 RESULTS AND DISCUSSION

In this paper, the thermo-electro-mechanical behavior of a functionally graded piezo-flexoelectric nano-plate was studied using a reformulated flexoelectric theory as explained in previous section. In this section, the results are determined considering the direct and inverse flexoelectric effects. Therefore, the displacement field, the electric potential function, the electric field function, and the polarization function for both direct and inverse flexoelectric effect are determined. It assumed that the functionally graded nano-plate is simply support on all edges.

Therefore, the effects of plate dimensions, the power law index related to the functionally graded behavior of FG material, applied electrical and mechanical loadings on the static bending of nano-plate are investigated. In this study, it is assumed that nano-plate is made up of PZT-5H, PZT-4 materials on the lower and upper surfaces, respectively. Due to the mentioned functionally graded model of nano-plate, the nano-plate material properties vary along the plate thickness based on the power law function. However, the properties of the top and bottom layers are constant. Properties of these materials are given in Table 1. [23-31-57]

PZT-4 material can be used to build high power acoustic radiating transducers due to high resistance to loss of polarization (depolarization), as well as a very low loss of dielectric properties under high electrical stimuli. The high power of this material in maintaining the state of polarization under mechanical stresses has made that PZT-4 to be very suitable for use in deep-submersion acoustic transducers as an active substance in electrical power generation systems [57].

The PZT-5H material can be used in hydrophones or instrumentation equipment for reasons including high resistivity at elevated temperatures, high sensitivity and long-term stability. Because including the low temperature of the Curie point, the working temperature range of this material is limited and with a better stability only at low temperatures (-300-0 °C) [57].

Also, the length scale parameters associated with the strain gradient are considered to be: $l_0 = l_1 = l_2 = l = 3 \times 10^{-8}$. In addition, the length scale parameters associated with electric polarization gradient, β_i , are assumed to be equal to 1 in some models.

5.1 Validation of results

In this section, the accuracy of the developed models is determined by comparing the present study results with the results of similar cases found in the literature. For this purpose, the results presented by Zhang et al. have been used [21]. It should be mentioned that the characteristics of BaTiO₃ are given in ref. [21]. Also, the displacement functions for the rectangular nano-plate with all edges clamped are presented by Ebrahimi and Barati [44]. These investigators have modeled the bending and free vibration of a BaTiO₃ flexoelectric nano-plate clamped on all edges. The results of presented models are compared with the reference results in Fig. 2. Note in this figure that obtained results are in good agreement with the reference results. Thus, the presented models are capable of predicting the static bending of the nano-plate with a good accuracy.

Table 1
Properties of PZT-4, PZT-5H materials.

	Elastic Constants ($\times 10^9 pa$)									Piezoelectric Coefficients(c/m^2)				
	C_{11}	C_{12}	C_{13}	C_{22}	C_{23}	C_{33}	C_{44}	C_{55}	C_{66}	e_{15}	e_{24}	e_{31}	e_{32}	e_{33}
PZT-4	139	77.8	74	139	74	115	25.6	25.6	30.6	10.5	10.5	-4.1	-4.1	14.1
PZT-5H	126	79.1	83.9	126	83.9	117	23	23	23.5	17	17	-6.5	-6.5	23.3
	Dielectric Constants ($\times 10^{-9} c / mV$)		Thermal Modulus ($\times 10^5 N / m^2 k$)		Flexoelectric Coefficients ($\times 10^{-6} c / m$)		Pyroelectric Coefficients ($\times 10^{-6} c / m^2 k$)							
	$\alpha_{11}=\alpha_{22}$	α_{33}	α_{11}^T	$\alpha_{33}^T = \alpha_{22}^T$	f_1	f_2	γ_1^T	γ_2^T						
PZT-4	5.84	7.124	4.738	4.529	2	1	25	25						
PZT-5H	15.052	13.015	4.27	-	0.10	0.5	5.48	5.48						
	Thermal Expansion Coefficients ($10^{-6} \times 1 / ^\circ K$)		Curie Point ($^\circ c$)		Density ($\times 10^3 kg / m^3$)									
	α_1		T_c		ρ									
PZT-4		1.923		328			7.5							
PZT-5H		9.6384		195			7.5							

In Fig. 2, our predictions of the induced electric field along the non-FGM nano-plate thickness direction, without the thermal effects are compared with the reference results. Note that, again, good agreement is observed between the results. This fact proves that the presented models can accurately predict the induced electric field in the non-FGM nano-plate as well.

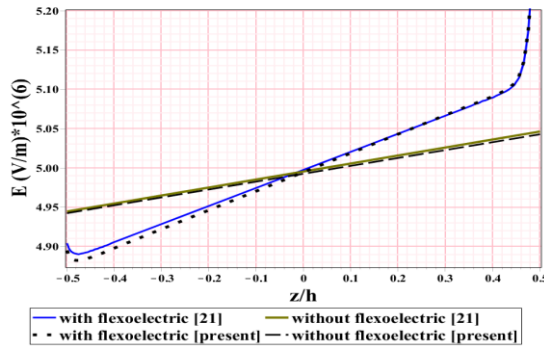


Fig.2
The electric field in terms of z/h ratio.

5.2 Effect of plate geometry and gradient index on the bending of flexoelectric nano-plate

After validation of our models, the direct flexoelectric effect on nano-plate behavior such as plate displacement, induced polarization, induced electric field, and induced electrical potential were determined. In Fig. 3, the deflection of the nano-plate at $y=b/2$ and the surface $z=0$ is depicted for different power law indices is shown. As can be seen in this figure, plate deflection decreases with increasing the power law index. This is due to the fact that an increase in n causes in an increase in the plate stiffness. In addition, the crystalline structure of the material along the z - direction changes as n increases, and the polarization changes along the thickness. By reducing the amount of polarization, the displacement caused by electrostatic force will also decrease.

In Fig. 4, the deflection of the plate is depicted considering the flexoelectric effect and without flexoelectric effect for $n=1$, $z=0$, $y=b/2$. It can be inferred from this figure that in the presence of flexoelectric effect, the displacement of the plate decreases. The reason seems to be that flexoelectric effect results in an increase in the plate stiffness.

The maximum deflection of the plate is shown in Fig. 5 with and without the flexoelectric effect at point $(a/2, b/2, 0)$ for $n=1$. These results also show the effects of the plate thickness. As can be seen, as the plate thickness increases, the maximum plate deflection decreases. According to this figure, the maximum plate deflections predicted by the two classic theories are close for thicknesses greater than $70 nm$. For plate thicknesses less than $50 nm$, the results of the two models show larger differences. Therefore, flexoelectricity plays a significant role in the electromechanical response of the plates with small thicknesses.

Maximum plate deflections in terms of the plate length to thickness ratio (a/h) are presented in Fig.6 for $n=1$ at point $(a/2, b/2, 0)$. Note that, at low length to plate thickness ratios, deflection increases slowly. At high values of this ratio, displacement increases sharply. Therefore, the maximum deflection increases with the increases in the plate length for constant values of the nano-plate thicknesses.

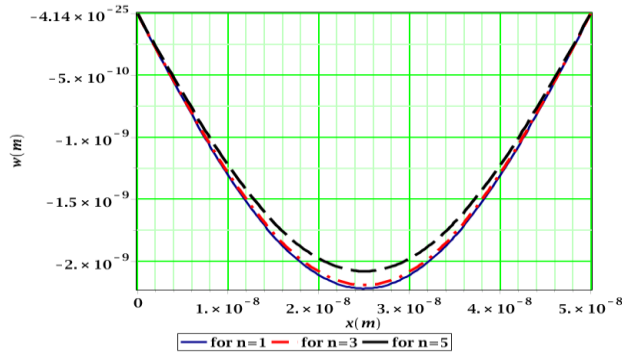


Fig.3 Deflection of FGM nano-plate along the x -direction for different values of FGM indices.

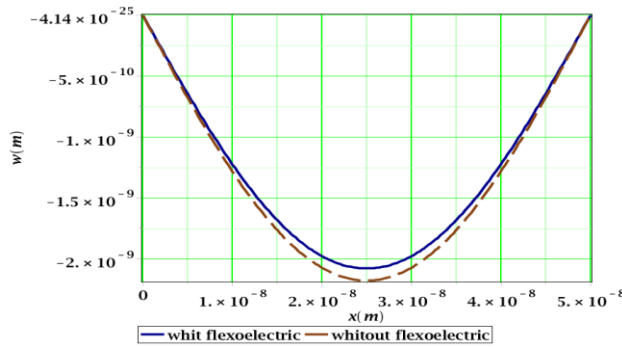


Fig.4 Deflection of FGM nano-plate along the x -direction with and without regarding the flexoelectric effect.

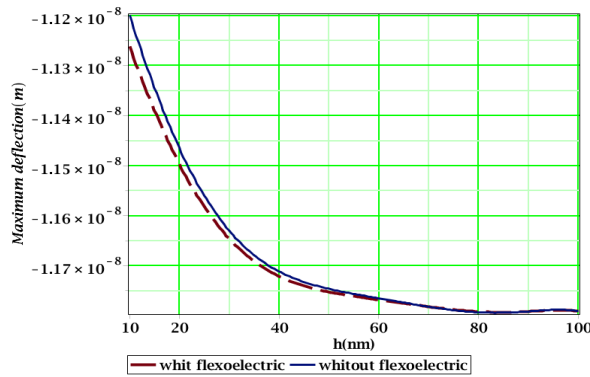


Fig.5 Maximum deflection of FGM nano-plate in terms of plate thickness with and without considering the flexoelectric effect.

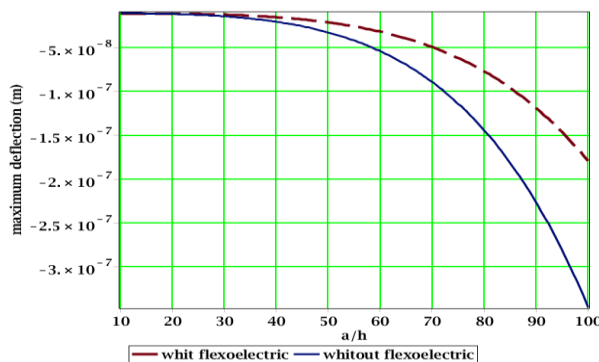


Fig.6 Maximum deflection of FGM nano-plate in terms of a/h ratios with and without considering the flexoelectric effect.

Fig. 7 shows the electric field for different values of the power law index associated to the functional behavior of the material (n) and for $h=400\text{ nm}$, along the z - direction, at the center of the nano-plate. Note that the induced electric field is minimum at the lower surface and increases in the plate thickness direction. Also, increasing the power law index results in a decrease in the induced electric field. The applied voltage is zero at the bottom surface and increases as we move towards the upper surface. Hence, the generated bipolarity increases along the plate thickness direction. As a result, the induced electric field also increases.

Fig. 8 shows the polarization variation along the plate thickness and different values of the length scale parameters related to polarization gradient (β) and $n=1$, at the center of the nano-plate. According to this figure, at low values of β , the polarization changes near the upper and lower surfaces of the plate rapidly. Also, the polarization in most layers along the thickness is almost constant. For large values of β , the polarization has steep variations near the upper and lower surfaces of the plate.

In Fig. 9, the polarization variation in terms of the thickness for $n=1$ at point $(a/2, b/2, 0)$ is shown. These results correspond to the two cases as with and without flexoelectric effect. As can be seen, increasing the plate thickness results in a decrease in the induced polarization. This is due to the fact that plate stiffness increases with thickness. In addition, polarization variation has a higher gradient for low thickness nano-plates.

The maximum nano-plate deflection along the thickness direction is shown in Fig.10 for different applied external voltages and $n=1$, at point $(a/2, b/2, 0)$. Note along the this figure that, the variation of maximum plate deflection is much smaller in high thickness nano-plates. Again, this suggests that the plate stiffness increases with increase the plate thickness. Finally, increasing the applied voltage, at constant thickness, results in an increase in the amount of bipolarity and eventually increases the plate deflection.

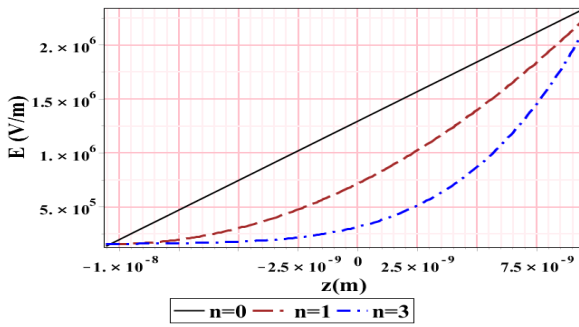


Fig.7
Electrical field along the plate thickness for different powers index of the FG plate.

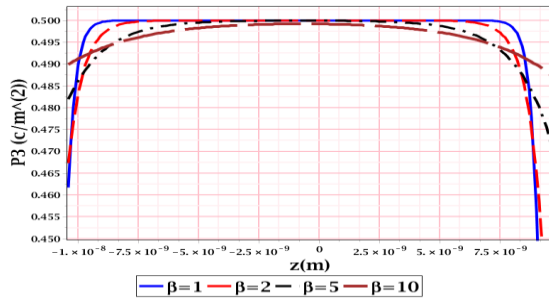


Fig.8
Polarization changes along the thickness for different values of β .

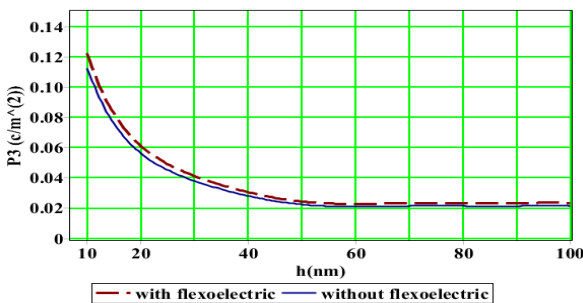


Fig.9
Polarization variations along thickness direction with and without flexoelectric.

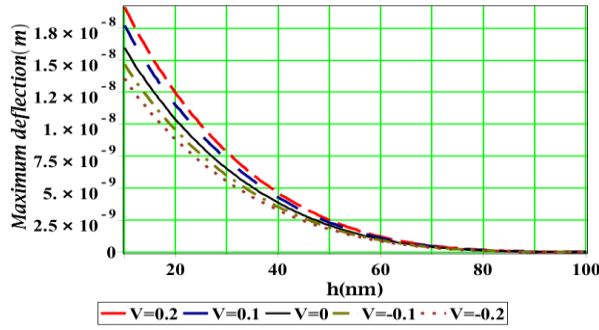


Fig.10
Maximum deflection in terms of thickness in the mode of inverse flexoelectric effect and different applied voltages.

In Fig. 11, the deflection curve is plotted along the thickness for $n=3$, $h=10 \text{ nm}$ and an applied voltage of $V=-0.1 \text{ v}$ at $z=0$. As is evident in this figure, the deflection is zero along the four edges of the plate. Due to the simply-supported boundary conditions, the deflection slope near the edges is non-zero. Finally, the maximum plate deflection occurs at the center of the nano-plate.

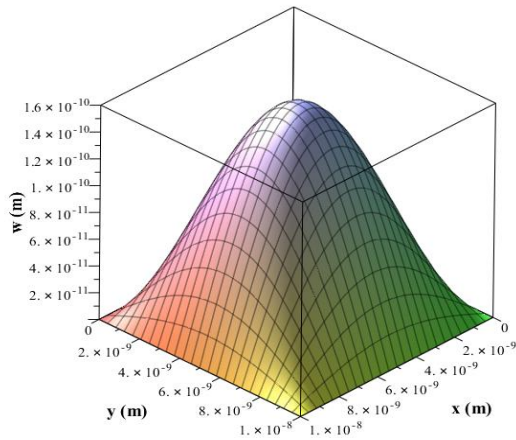


Fig.11
Deflection along the plate thickness direction in the inverse flexoelectric effect case.

Fig. 12 shows the polarization variation along the plate thickness for $n=3$ under the applied voltages 0.1 and -0.1volts. These results correspond to the points $(x,y) = (0, b/2)$ and $(x,y) = (a/2, b/2)$, at $z = 0$. The analyses were performed the classical model without flexoelectric effect. These results suggest that increasing the nano-plate thickness results in a decrease in the polarity. Also, variations of polarization are approximately zero for high nano-plate thickness. Note that, with increasing the plate thickness, its rigidity increases, thus the plate displacement and induced polarization decreases. Changing the applied voltage sign, the direction of the bipolar vectors is inverted.

In Fig. 13, distributions of polarization on the $z=0$ surface are plotted for $n= 3$ and $h=10 \text{ nm}$. The polarization is zero along the edges of the plate with a maximum value at the center.

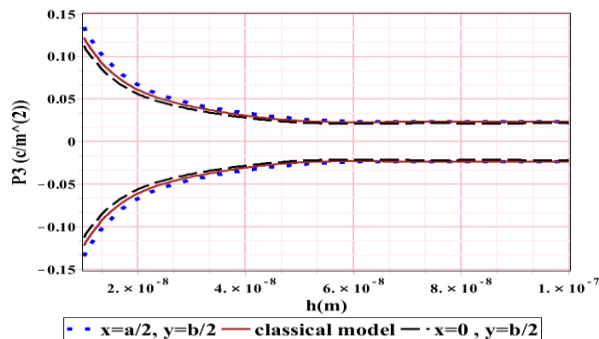


Fig.12
Polarization variation along the plate thickness in the neutral plan for $h=20 \text{ nm}$ with applied voltage $V_0=0.1 \text{ v}$, -0.1v.

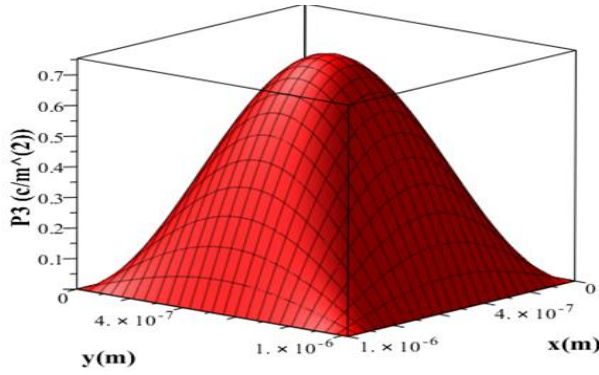


Fig.13
3-D Polarization variations on the neutral plan with applied voltage $V_0 = -0.1v$.

Fig. 14, shows the polarization variations in terms of temperature for different power law indices of the functionally graded nano-plate at point $(a/2, b/2, 0)$. These results indicate that increasing the nano-plate temperature results in an increase in the reaction forces along the plate edges. These reaction forces result in an additional plate deflection, which is much smaller than the deflections resulting from the other loadings. At temperatures near the material Curie point the material crystalline structure collapses, thus its magnetic and electrical properties of the material degrade [58]. At temperatures below the material Curie point, increasing the temperature results in a reduction in polarization. This is due to the fact that increasing temperature results in an increase in nano-plate deflection. Thus, strain gradient in the nano-plate decreases.

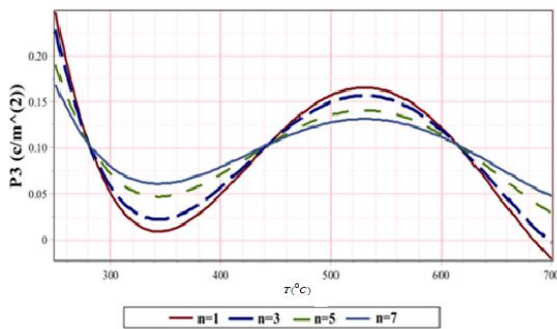


Fig.14
Variations of Polarization in terms of the temperature on the neutral plane for $h=10\text{ nm}$ with applied voltage of $V_0 = -0.1v$.

Fig. 15 shows the maximum plate deflection in terms of the temperature for different h/l ratios and $n=1$ at point $(a/2, b/2, 0)$. Note in this figure that, maximum plate deflection increases slightly in terms of the temperature.

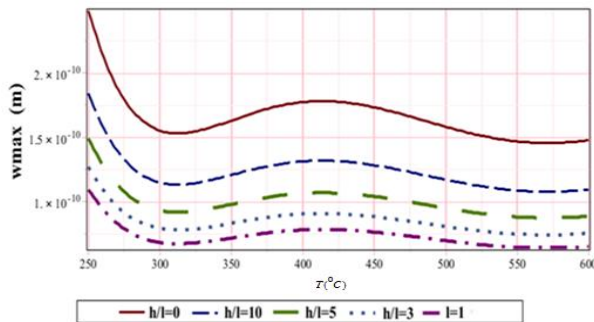


Fig.15
Variations of the maximum deflection in terms of the temperature for $h=10\text{ nm}$ with applied voltage of $V_0 = -0.1v$.

6 CONCLUSIONS

In this paper, static analysis of the functionally graded piezo-flexoelectric nano-plate under electro-thermo-mechanical loadings was performed. Based on the obtained results in this investigation, the following conclusions can be drawn:

1. Flexoelectric nano-plate has a lower displacement than nano-plate without flexoelectric effect.
2. Increasing the power law index, associated with functional behavior of the nano-plate, results in a decrease in nano-plate deflection.
3. Nano-plate deflection in both direct and inverse flexoelectric effect decreases with increasing the nano-plate thickness.
4. Increasing the nano-plate thickness results in a decrease in polarization of the nano-plate. Thus, polarization gradient is almost zero in high thickness plates.
5. Changing the applied voltage sign reverses the induced electric field and polarization vectors direction.
6. Increasing the length scale parameter related to the polarization gradient (β), the polarization decreases along the nano-plate thickness direction. Also, polarization gradient in the regions near the nano-plate neutral plane decreases.
7. As temperature increases, polarization decreases. Conversely, nano-plate deflection increases with temperature.
8. Increasing the length scale parameters, associated with strain gradient (l_i), the amount of displacement and polarization increases.

REFERENCES

- [1] Lao C.S., Kuang Q., Wang Z. L., Park M.C., Deng Y.L., 2007, Polymer functionalized piezoelectric-FET as humidity/chemical nanosensors, *Applied Physics Letters* **90**: 262107.
- [2] Tanner S.M., Gray J.M., Rogers C.T., Bertness K.A., Sanford N.A., 2007, High-Q GaN nanowire resonators and oscillator, *Applied Physics Letters* **91**: 203117.
- [3] Kogan S.M., 1996, Piezoelectric effect during inhomogeneous deformation and acoustic scattering of carriers in crystals, *Soviet Physics, Solid State* **5**: 2069-2070.
- [4] Majdoub M.S., Sharma P., Cagin T., 2008, Enhanced size-dependent piezoelectricity and elasticity in nanostructures due to the flexoelectric effect, *Physical Review B* **77**: 125424.
- [5] Kogan S.M., 1963, Piezoelectric effect under an inhomogeneous strain and acoustic scattering of carriers in crystals, *Fizika Tverdogo Tela* **5**: 2829-2831.
- [6] Maranganti R., Sharma N.D., Sharma P., 2006, Electromechanical coupling in nonpiezoelectric materials due to nanoscale nonlocal size effects: Green's function solutions and embedded inclusions, *Physical Review B* **74**: 014110.
- [7] Shen S.P., Hu S.L., 2010, A theory of flexoelectricity with surface effect for elastic dielectrics, *Journal of the Mechanics and Physics of Solids* **58**: 665-677.
- [8] Yan Z., Jiang L.Y., 2013, Flexoelectric effect on the electroelastic responses of bending piezoelectric nano-beams, *Journal of Applied Physics* **113**: 194102.
- [9] Yan Z., Jiang L.Y., 2013, Size-dependent bending and vibration behavior of piezoelectric nano-beams due to flexoelectricity, *Journal of Physics D: Applied Physics* **46**: 355502.
- [10] Li A., Zhou S., Qi L., Chen X., 2015, A reformulated flexoelectric theory for isotropic dielectrics, *Journal of Physics D: Applied Physics* **48**(46): 465202.
- [11] Xu Y.M., Shen H.S., Zhang C.L., 2013, Nonlocal plate model for nonlinear bending of bilayer graphene sheets subjected to transverse loads in thermal environment, *Composite Structures* **98**: 294-302.
- [12] Chen Y., Lee J.D., Eskandarian A., 2004, Atomistic viewpoint of the applicability of microcontinuum theories, *International Journal of Solids Structures* **41**(8): 2085-2097.
- [13] Li A.Q., Zhou S.J., Zhou S.S., Wang B.L., 2014, Size-dependent analysis of a three-layer micro-beam including electromechanical coupling, *Composite Structures* **116**: 120-127.
- [14] Hadesfandiari A.R., 2013, Size-dependent piezoelectricity, *International Journal of Solids Structures* **50**: 2781-2791.
- [15] Liang X., Shen S.P., 2013, Size-dependent piezoelectricity and elasticity due to the electric field-strain gradient coupling and strain gradient elasticity, *International Applied Mechanics* **5**: 1350015.
- [16] Hu S.L., Shen S.P., 2009, Electric field gradient theory with surface effect for nano-dielectrics, *Computers, Materials and Continua* **13**: 63-87.
- [17] Yang J.S., 1999, Equations for the extension and flexure of electroelastic plate under strong electric fields, *International Journal of Solids Structures* **36**: 3171-3192.
- [18] Liu C., Ke L.L., Wang Y.S., Yang J., Kitipornchai S., 2013, Thermo-electro mechanical vibration of piezoelectric nano-plate based on the nonlocal theory, *Composite Structures* **106**: 167-174.

- [19] Yan Z., Jiang L.Y., 2011, Electromechanical response of a curved piezoelectric nano-beam with the consideration of surface effects, *Journal of Physics D: Applied Physics* **44**: 365301.
- [20] Ke L.L., Wang Y.S., 2012, Thermo-electric-mechanical vibration of piezoelectric nano-beams based on the nonlocal theory, *Smart Materials and Structures* **21**(2): 025018.
- [21] Zhang Z., Yan Z., Jiang L., 2014, Flexoelectric effect on the electroelastic responses and vibrational behaviors of a piezoelectric nano-plate, *Journal of Applied Physics* **116**(1):014307.
- [22] Zhang Z., Jiang L., 2014, Size effects on electromechanical coupling fields of a bending piezoelectric nano-plate due to surface effects and flexoelectricity, *Journal of Applied Physics* **116**(13): 4308.
- [23] Yang W., Liang X., Shen S., 2015, Electromechanical responses of piezoelectric nano-plate with flexoelectricity, *Acta Mechanica* **226**: 3097-3110.
- [24] Yan Z., Jiang L.Y., 2012, Vibration and buckling analysis of a piezoelectric nano-plate considering surface effects and in-plane constraint, *Proceedings of the Royal Society of Series A* **468**: 3458-3475.
- [25] Yan Z., Jiang L.Y., 2013, Size-dependent bending and vibration behavior of piezoelectric nano-beams due to flexoelectricity, *Journal of Physics D: Applied Physics* **46**: 355502.
- [26] Murmua T., Sienz J., Adhikari S., Arnold C., 2013, Nonlocal buckling of double-nano-plate-systems under biaxial compression, *Composites Part B* **44**: 84-94.
- [27] Li Y.S., Cai Z.Y., Shi S.Y., 2014, Buckling and free vibration of magneto electroelastic nano-plate based on nonlocal theory, *Composite Structures* **111**: 522-529.
- [28] Liang X., Hu S., Shen S., 2014, Effects of surface and flexoelectricity on a piezoelectric nano-beam, *Smart Materials and Structures* **23**: 035020.
- [29] Liang X., Shuling H., Shengping S., 2015, Size-dependent buckling and vibration behaviors of piezoelectric nanostructures due to flexoelectricity, *Smart Materials and Structures* **24**: 105012.
- [30] Yan Z., Jiang L.Y., 2015, Effect of flexoelectricity on the electroelastic fields of a hollow piezoelectric nanocylinder, *Smart Materials and Structures* **24**: 065003.
- [31] Ke L., Liu C., Wang Y.S., 2015, Free vibration of nonlocal piezoelectric nano-plate under various boundary conditions, *Physica E* **66**: 93-106.
- [32] Liu C., Ke L.L., Wang Y.S., Yang J., Kitipornchai S., 2013, Thermo-electro-mechanical vibration of piezoelectric nano-plate based on the nonlocal theory, *Composite Structures* **106**: 167-174.
- [33] Liang X., Yang W., Hu S., Shen S., 2016, Buckling and vibration of flexoelectric nanofilms subjected to mechanical loads, *Journal of Physics D: Applied Physics* **49**: 115307.
- [34] Alibeigi E., Tadi Beni Y., Mehralian F. 2018, Thermal buckling of magneto-electro- elastic piezoelectric nano-beams based on the modified couple stress theory, *The European Physical Journal Plus* **133**: 133.
- [35] Komijani M., Kiani Y., Esfahani S., Eslami M., 2013, Vibration of thermo-electrically post-buckled rectangular functionally graded piezoelectric beams, *Composite Structures* **98**: 143-152.
- [36] Komijani M., Reddy J., Eslami M., 2014, Nonlinear analysis of microstructure-dependent functionally graded piezoelectric material actuators, *Journal of the Mechanics and Physics of Solids* **63**: 214-227.
- [37] Xiang H.J., Shi Z., 2009, Static analysis for functionally graded piezoelectric actuators or sensors under a combined electrothermal load, *European Journal of Mechanics A* **28**: 338-346.
- [38] Yang J., Xiang H., 2007, Thermo-electro-mechanical characteristics of functionally graded piezoelectric actuators, *Smart Materials and Structures* **16**: 784.
- [39] Tadi Beni Y., 2016, A nonlinear electro-mechanical analysis of nano-beams based on the size-dependent piezoelectricity, *Journal of Mechanics* **33**: 289-301.
- [40] Ke L.L., Wang Y.S., Yang J., Kitipornchai S., 2014, Free vibration of size-dependent magneto-electro-elastic nano-plate based on the nonlocal theory, *Acta Mechanica Sinica* **30**: 516-525.
- [41] Ke L.L., Wang Y.S., Reddy J.N., 2014, Thermo-electro-mechanical vibration of size-dependent piezoelectric cylindrical nanoshells under various boundary conditions, *Composite Structures* **116**: 626-636.
- [42] Kiani Y., Taheri S., Eslami M.R., 2011, Thermal buckling of piezoelectric functionally graded material beams, *Journal of Thermal Stresses* **34**: 835-850.
- [43] Kiani Y., Rezaei M., Taheri S., Eslami M.R., 2011, Thermo-electrical buckling of piezoelectric functionally graded material Timoshenko beams, *International Journal of Mechanics and Materials in Design* **7**: 185-197.
- [44] Ebrahimi F., Barati M.R., 2017, Vibration analysis of size-dependent flexoelectric nano-plates incorporating surface and thermal effects, *Journal of Mechanics of Advanced Materials and Structures* **25**: 611-621.
- [45] Ebrahimi F., Barati M.R., 2017, Modeling of smart magnetically affected flexoelectric/piezoelectric nanostructures incorporating surface effects, *Nanomaterials and Nanotechnology* **7**(2): 1-11.
- [46] Ebrahimi F., Ehyaei J., Babaei R., 2016, Thermal buckling of FGM nano-plates subjected to linear and nonlinear varying loads on Pasternak foundation, *Advanced in Materials Research* **5**: 245-261.
- [47] Ebrahimi F., Salari E., 2015, Size-dependent thermo-electrical buckling analysis of functionally graded piezoelectric nano-beams, *Smart Materials and Structures* **24**: 125007.
- [48] Ebrahimi F., Barati M.R., 2016, An exact solution for buckling analysis of embedded piezo- electro-magnetically actuated nanoscale beams, *Advances in Nano Research* **4**: 65-84.

- [49] Ebrahimi F., Barati M.R., 2017, Surface effects on the vibration behavior of flexoelectric nanobeams based on nonlocal elasticity theory, *The European Physical Journal Plus* **132**: 11320.
- [50] Ebrahimi F., Barati M.R., 2016, Electromechanical buckling behavior of smart piezoelectrically actuated higher-order size dependent graded nanoscale beams in thermal environment, *International Journal of Smart and Nano Materials* **7**: 69-90.
- [51] Tadi Beni, Y., 2016, Size-dependent analysis of piezoelectric nano-beams including electro-mechanical coupling, *Mechanics Research Communications* **75**: 67-80.
- [52] Shen S.P, Hu S.L., 2010, A theory of flexoelectricity with surface effect for elastic dielectrics, *Journal of the Mechanics and Physics of Solids* **58**: 665-677.
- [53] Eliseev E.A., Morozovska A.N., Glinchuk M.D., Blinc R., 2009, Spontaneous flexoelectric-flexomagnetic effect in nanoferroics, *Physical Review B* **79**: 165433.
- [54] Li J.U., 2004, The effective pyroelectric and thermal expansion coefficients of ferroelectric ceramics, *Mechanics of Material* **36**: 949-958.
- [55] Toupin R.A., 1956, The elastic dielectric, *Rational Mechanics and Analysis* **5**: 849-915.
- [56] Tadi Beni Y., Mehralian F., Razavi H., 2015, Free vibration analysis of size-dependent shear deformable functionally graded cylindrical shell on the basis of modified couple stress theory, *Composite Structures* **120**: 65-78.
- [57] Mehralian F., Tadi Beni Y., 2016, Ansari R., Size dependent buckling analysis of functionally graded piezoelectric cylindrical nanoshell, *Journal of Composite Structures* **152**: 45-61.
- [58] Fei L., Zhuo X., Xiaoyong W., Xi Y., 2009, Determination of temperature dependence of piezoelectric coefficients matrix of lead zirconate titanate ceramics by quasi-static and resonance method, *Journal of Physics D: Applied Physics* **42**: 095417.